Molecular Crystals and Liquid Crystals

ISSN: 1542-1406 (Print) 1563-5287 (Online) Journal homepage: http://www.tandfonline.com/loi/gmcl20

Asymmetric Director Structures and Ions in the Measurement of the Flexoelectric Sum ($e_1 + e_3$)

Chloe C. Tartan & Steve J. Elston

Mol. Cryst. Liq. Cryst., Vol. 610: pp. 77–88, 2015

ISSN: 1542-1406 print/1563-5287 online
DOI: 10.1080/15421406.2015.1025209

Asymmetric Director Structures and Ions in the Measurement of the Flexoelectric Sum ($e_1 + e_3$)

CHLOE C. TARTAN* AND STEVE J. ELSTON

Department of Engineering Science, University of Oxford, Oxford, United Kingdom

Hybrid Aligned Nematic (HAN) devices filled with highly ionic liquid crystal materials screen out the internal bias due to surface polarization, making it possible to determine the flexoelectric sum, $e_1 + e_3$*. A transient change is observed in the device response due to differing polarities of an external offset applied to an AC signal, with a time constant similar to the characteristic ion relaxation time in the material. Assuming ions screen out the internal bias, data-theory fits in the low frequency, low voltage perturbative regime gives a value of* $|e_1 + e_3| = 10\ pCm^{-1}$ *for the standard commercial eutectic E70 nematic liquid crystal mixture.*

Keywords liquid crystal; flexoelectricity; hybrid aligned nematic; display technology; photonic technology

Introduction

Liquid crystal (LC) devices that have asymmetry in their molecular alignment resultant from a mechanical deformation of the director field ($\hat{n}$) lead to a net electric polarization. This induced field is related to the flexoelectric effect, which has shown high speed switching in LC devices for potential applications in field sequential colour display technologies. However, the difficulty in determining the flexoelectric coefficients that quantify these interesting electro-optic properties is one of the main obstacles preventing its exploitation as a commercial photonic technology.

Flexoelectricity is attributed to the shape asymmetry and permanent dipole moments of LC molecules. Constraining a system of molecules with longitudinal dipoles to a splay geometry induces a net flexoelectric polarization, which is described in magnitude and direction by the splay flexoelectric coefficient (e_1). Similarly, the bend flexoelectric coefficient (e_3) defines the polarization induced from molecular systems with transverse dipoles when confined to bend geometries [1]. Using the original Meyer convention, the total flexoelectric polarization can be written as[1],

---

*Address correspondence to Chloe C. Tartan, Department of Engineering Science, University of Oxford, Parks Road, Oxford, OX1 3PJ, United Kingdom. E-mail: chloe.tartan@eng.ox.ac.uk

[1]In some published work the flexoelectric polarization is defined as $P = e_s\hat{n} \cdot (\nabla \cdot \hat{n} + e_b\hat{n})$ [2]. Here we have used the original definition introduced by Meyer in 1969 [1]. The two notations are equivalent with $e_s = e_1$ and $e_b = -e_3$.

Color versions of one or more of the figures in the article can be found online at www.tandfonline.com/gmcl.

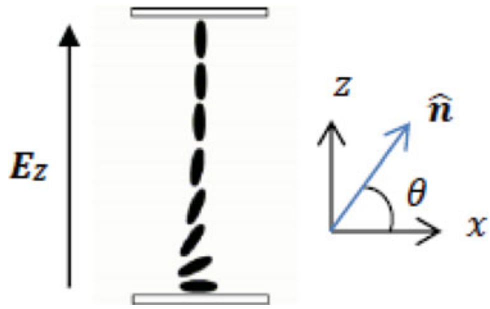

Figure 1. Schematic of director structure in HAN device.

$$\boldsymbol{P}_f = e_1 \hat{\boldsymbol{n}} \cdot (\nabla \cdot \hat{\boldsymbol{n}}) + e_3 (\nabla \times \hat{\boldsymbol{n}}) \times \hat{\boldsymbol{n}}. \tag{1}$$

A hybrid aligned nematic (HAN) device as shown in Fig. 1 results in homeotropic molecular alignment at one boundary surface and homogeneous planar alignment at the other [2]. Confining the director, which represents the LC molecular alignment, to a HAN geometry causes a strong splay-bend distortion field due to the asymmetry in the molecular distribution, which is potentially useful for the measurement of flexoelectric polarization.

An electric field applied parallel in the plane of the director along the z-axis (E_z) couples to the sum of the flexoelectric coefficients, and a positive dielectric anisotropy LC material tends to align the molecules in the direction of the field in the HAN geometry. Writing the director field in terms of the tilt angle that defines the orientation of the director field in the xz plane(θ) gives the free energy density due to flexoelectricity as,

$$f_{flexo} = -\boldsymbol{P_f} \cdot \boldsymbol{E} = -\frac{1}{2}(e_1 + e_3)\sin(2\theta)\frac{\partial\theta}{\partial z}E_z. \tag{2}$$

The flexoelectric polarization in (1) gives rise to a bulk torque on the director field [2], which is given in terms of the molecular field as,

$$\boldsymbol{\Gamma}^{\mathrm{b}}_{\mathrm{flexo}} = \hat{n} \times h_f, \tag{3}$$

where

$$\boldsymbol{h}_f = (e_1 - e_3)[\boldsymbol{E}(\nabla\cdot\hat{\boldsymbol{n}}) - (\nabla \otimes \hat{\boldsymbol{n}})\boldsymbol{E}] - (e_1 + e_3)(\hat{\boldsymbol{n}} \cdot \nabla)\boldsymbol{E}. \tag{4}$$

For a HAN structure with an applied electric field parallel to the plane of the director, the torque dependent on the difference of the flexoelectric coefficients cancels. The remaining second term in (4) is related to field gradients due to the dielectric effect coupled to the sum of the flexoelectric coefficients, giving a resultant bulk flexoelectric torque as,

$$\boldsymbol{\Gamma}^{\mathrm{b}}_{\mathrm{flexo}} = -\frac{1}{2}(e_1 + e_3)\sin(2\theta)\frac{\partial E_z}{\partial z} \tag{5}$$

Numerical Model of a HAN Cell

Flexoelectricity is attributed to sign-dependent responses on account of its linear dependence on the applied electric field, while the dielectric effect is largely sign-independent as it is quadratic in the applied field. Therefore the internal flexoelectric field either enhances or suppresses the dielectric response of the cell, depending on the polarity of the applied field. This can be shown by simulating the director profiles from a HAN device under the application of forward and reverse bias DC voltages. A model of the HAN structure can be written in terms of the director field as a function of the tilt angle, $\hat{\boldsymbol{n}} = \boldsymbol{n}(\theta)$. The elastic, dielectric and flexoelectric energy density terms are given by,

$$\begin{aligned} f_{elastic} &= \frac{1}{2}\left\{K_{11}(\nabla\cdot\hat{\boldsymbol{n}})^2 + K_{22}(\hat{\boldsymbol{n}}\cdot\nabla\times\hat{\boldsymbol{n}})^2 + K_{33}(\hat{\boldsymbol{n}}\times\nabla\times\hat{\boldsymbol{n}})^2\right\}, \\ f_{dieletric} &= -\frac{1}{2}\boldsymbol{D}\cdot\boldsymbol{E} = -\frac{1}{2}D_z\cdot E_z = -\frac{1}{2}\varepsilon_0\varepsilon_{zz}E_z^2, \\ f_{flexo} &= -\frac{1}{2}(e_1+e_3)\sin 2\theta\frac{\partial\theta}{\partial z}E_z, \end{aligned} \tag{6}$$

where $\varepsilon_{zz} = \varepsilon_\perp + \Delta\varepsilon\,\sin^2\theta$. Neglecting changes occurring in the x and y directions, and initially assuming there are no free charges, the non-uniform electric field that appears in the dielectric energy density in (6) can be written in terms of a constant displacement field (D_z),

$$E_z = \frac{D_z - P_f}{\varepsilon_0\varepsilon_{zz}}. \tag{7}$$

The potential applied across the cell is then derived as follows;

$$\begin{aligned} -V &= \int_0^d E_z dz \\ &= \int_0^d \frac{D_z - P_f}{\varepsilon_0\varepsilon_{zz}} dz \\ &= \frac{1}{\varepsilon_0}\left(D_z\int_0^d \frac{1}{\varepsilon_{zz}}dz - \int_0^d \frac{P_f}{\varepsilon_{zz}}dz\right). \end{aligned} \tag{8}$$

Rearranging (16) gives an expression for the displacement field,

$$D_z = \frac{-\varepsilon_0 V + \int_0^d \frac{P_f}{\varepsilon_{zz}}dz}{\int_0^d \frac{1}{\varepsilon_{zz}}dz}, \tag{9}$$

which can be substituted back into (7) in order to calculate the local electric field along the z-axis. The model uses a finite difference of the Euler Lagrange equation to determine the minimization of the free energy terms in (6), which is equated to a viscous dissipation

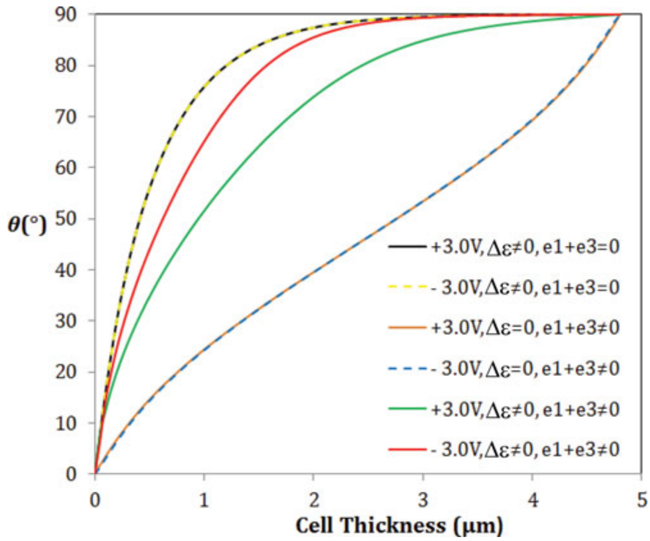

Figure 2. Simulated director profiles from a HAN device under the application of a ±3V DC field when the dielectric effect, the flexoelectric effect, or both effects are included in the model.

term;

$$-\left(K_{11}\cos^2\theta + K_{33}\sin^2\theta\right)\left(\frac{\partial^2\theta}{\partial z^2}\right) + \frac{1}{2}\left\{(K_{11} - K_{33})\left(\frac{\partial\theta}{\partial z}\right)^2 - \varepsilon\varepsilon_0 E_z^2 + (e_1 + e_3)\left(\frac{\partial E_z}{\partial z}\right)\right\}\sin 2\theta = -\gamma\frac{\partial\theta}{\partial t}. \tag{10}$$

Figure 2 shows the output from the model under various conditions for an applied voltage of ±3V. Removing flexoelectric contributions altogether ($e_1 + e_3 = 0$) reveals an identical dielectric response when changing the polarity of the applied voltage (black and dotted yellow lines). In the absence of dielectric anisotropy ($\Delta\varepsilon = 0$), identical director profiles result for both signs of the applied field (orange and blue dotted lines) under the flexoelectric effect. This is in accordance with the relation for the bulk flexoelectric torque in (5), which relies on field gradients to allow the coupling of flexoelectricity to an external field. However, the curvature of the director profile in this instance reveals self-coupling to the internally induced flexoelectric field. When both dielectric and flexoelectric effects are included in the model ($\Delta\varepsilon \neq 0$, $e_1 + e_3 \neq 0$), the flexoelectric polarization couples to the external field and enhances the dielectric response under a positive field (red line), while suppressing the response under a negative applied field (green line).

Internal Bias

The HAN geometry is achieved by treating the two surfaces asymmetrically, forming planar alignment at one substrate and homeotropic at the other. The resultant different surface alignment polarities induce an effective voltage shift, which we refer to as an internal bias (V_b). Approximating the flexoelectric polarization to a small perturbation on the field in a cell and simplifying the expressions for energy and torque, the importance of small voltage offsets on the flexoelectric effect can be shown analytically.

Ignoring the small internal flexoelectric field, (7) and (8) can be simplified using the following expression for the displacement field,

$$D_z = \varepsilon_0 \varepsilon E_z \Rightarrow E_z = \frac{D_z}{\varepsilon_0 \varepsilon} \Rightarrow V = -\frac{D_z}{\varepsilon_0} \int^{\frac{1}{\varepsilon}}. \tag{11}$$

The field gradient is derived by rearranging for D_z and substituting back into (11), which differentiates to give

$$\frac{\partial E_z}{\partial z} = \frac{V}{\varepsilon^2 \int \frac{1}{\varepsilon}} \frac{\partial \varepsilon}{\partial z}, \tag{12}$$

where $\int \frac{1}{\varepsilon} \approx \frac{d}{\varepsilon_{\mathrm{AV}}}$ for small dielectric anisotropy($\Delta\varepsilon$). Setting $\partial\varepsilon$ as the difference between the z-components of the relative dielectric permittivity at the device boundaries and assuming a uniform change between the two substrates, a useful approximation to the field gradient in the device is obtained as,

$$\frac{\partial E_z}{\partial z} = \frac{V}{\varepsilon_{\mathrm{AV}}^2 \left\{ \frac{d}{\varepsilon_{\mathrm{AV}}} \right\}} \frac{\partial \varepsilon}{d} = \frac{V \partial \varepsilon}{\varepsilon_{\mathrm{AV}} d^2}. \tag{13}$$

Applying a total voltage of $V = V_a + V_b$ (the summation of an applied and offset bias voltage), the field gradient approximation in (14), leads to the following simplified torque approximations;

$$diel_{torque} \approx \frac{\varepsilon \varepsilon_0}{d^2} \left(V_a^2 + 2 V_a V_b + V_a^2 \right), \tag{14}$$

$$flexo_{torque} \approx e \left(V_a + V_b \right) \frac{\partial \varepsilon}{\varepsilon_{AV} d^2}. \tag{15}$$

where e is a measure of flexoelectricity. Gathering dielectric and flexoelectric terms that grow linearly with the appliedV_a, the total torque in a HAN cell can be written in first order terms with respect to the applied voltage V_a as,

$$Total \approx \frac{\varepsilon V_a}{d^2} \left\{ 2\varepsilon_0 V_b + \frac{e}{\varepsilon_{\mathrm{AV}}} \right\}. \tag{16}$$

Equating the terms in the brackets to find an equivalent value of the flexoelectric effect for an offset voltage gives,

$$e_{equivalent} \approx 2\varepsilon_0 V_b \varepsilon_{\mathrm{AV.}} \tag{17}$$

The expression in (17) highlights that linear reorienting torques can occur equivalently due to the presence of flexoelectricity or a (potentially unknown) bias voltage, and (18) highlights that for any possible bias voltage there is an equivalent (indistinguishable)

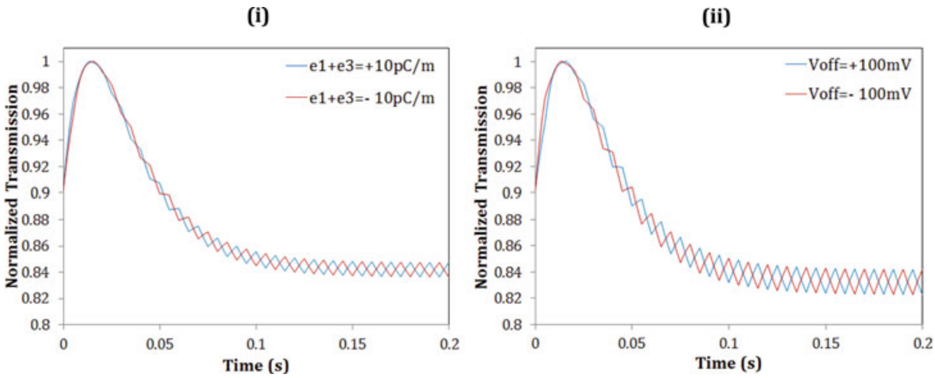

Figure 3. Simulated transmission as a function of time from HAN device under the application of a 100 Hz, ±1.0 Vrms square wave with (i) a flexoelectric sum of $e_1 + e_3 = \pm 10$ pCm^{-1} ($V_{\text{off}} = 0$) and (ii) an external DC offset of ±100 mV ($e_1 + e_3 = 0$).

flexoelectricity, and vice-versa. Interestingly, this is of course also equivalent to the effective internal bias due to flexoelectricity in [3], the two equations being the same for small $\Delta\varepsilon$. The importance, and potential problem, of small bias voltage offsets then becomes evident from both expressions, which with typical dielectric parameters gives an equivalent flexoelectric coefficient of ~10 pCm^{-1} for an offset of just 100 mV (and vice-versa). This reinforces the potential impact of small offsets due to surface polarity when measuring flexoelectric effects, which can be very significant.

The relation in (18) can be used to calculate an estimate for the effective internal bias due to the induced surface and flexoelectric polarizations. In the absence of flexoelectricity, deliberately applying an external DC offset to the voltage using this estimate should demonstrate the equivalence between flexoelectricity and bias. Fig. 3 shows a comparison between the theoretical transmission against time from a HAN device under the application of 100 Hz, ±1.0 Vrms square wave, when either a flexoelectric sum of ±10 pC/m is included in the model and no external offset is applied (Fig. 3.i.), or the signal is offset by ±100 mV in the absence of flexoelectricity (Fig. 3.ii.). Despite the slight differences in the amplitude of the modulation along with the equilibrium transmission level, both plots show the same behaviour. This highlights the identical behaviour between flexoelectricity and internal bias due to surface polarity (assuming it is a similar order of magnitude to the external offset applied here), and the difficulties in distinguishing between the two for a measurement of the flexoelectric coefficients.

Ionic Screening

The work carried out in the current investigation supports the discussions presented by Ponti et al. [3] and Barbero and Evangelista [4], insofar as the measurement of the flexoelectric coefficients is potentially skewed by the internal bias that arises from the different surface alignment polarities in the HAN geometry, and is further complicated by the presence of the ions. Moreover, ionic screening in HAN cells has previously only been considered in complex waveguide systems [5].

Figure 4.i shows the simulated response under the application of a 100 Hz, ±0.2 Vrms square wave offset by ±200 mV, with a flexoelectric sum fixed at an arbitrary value of 60 pCm^{-1}. The modulated flexoelectric response is reinforced for one polarity of the applied

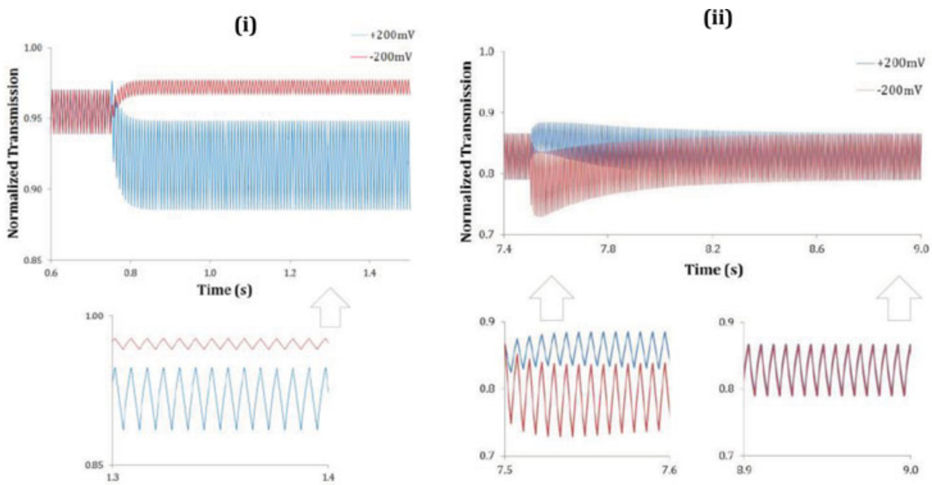

Figure 4. Simulated transmission as a function of time from HAN device under the application of a ±200 mV external DC offset to a 100 Hz, 0.2 V square wave and $e_1 + e_3 = 60$ pCm^{-1} with (i) no ionic contribution and (ii) pseudo-ions added to the model as a general screening effect.

external offset and cancelled for the other, leading to an increase/decrease in transmission with positive/negative step changes. The same is true when fixing the external offset and changing the polarity of the sum of flexoelectric coefficients.

The simulated response of the HAN cell due to step changes in the external offset when ionic screening is added to the model is shown in Fig. 4.ii. The ions are implemented as a general screening effect using a single time constant that is set by observing the transport across the device, and the field due to the ions is then subtracted from the field calculated in (7). Varying the offset causes a transient change in the response from the cell, with each plot returning to its equilibrium transmission over time. As the ions apparently drift to screen out any external changes in offset voltage, *it is also reasonable to assume that they drift to screen out any internal bias voltage*. Therefore the response to low frequency signals may be useful for the measurement of the flexoelectric response.

Experimental Arrangement

The optical set-up as shown in Fig. 5 illustrates the beam trajectory (red) of monochromatic light (wavelength 632.8nm) emitted from a class 3R HeNe laser. Light is transmitted to the test cell, which is between cross polarizers. The device is perpendicular to the laser beam, but oriented so that the director is angled at 45° to the plane of polarization (polarizer and

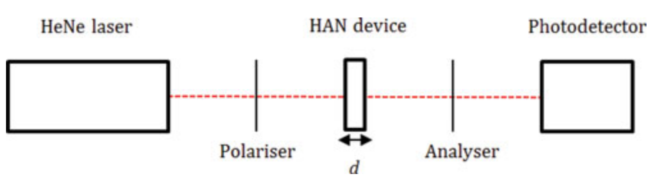

Figure 5. Optical set-up for the measurement of the flexoelectric sum in the E70 nematic LC mixture.

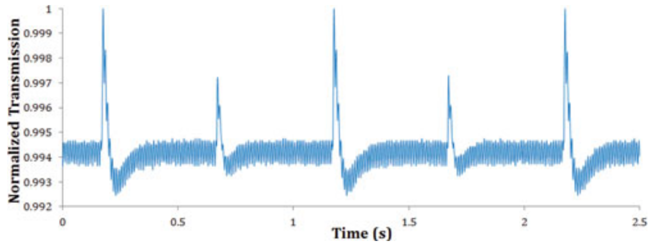

Figure 6. Transient E70 LC response to 100 Hz, ±0.1 Vrms field offset by a 1 Hz, ±200 mV square wave.

analyzer) for maximum transmission. The signal is detected at a photodiode and observed on an oscilloscope.

Figure 6 shows the transmission as a function of time obtained from the experimental arrangement described above, when driving the device with a 100 Hz, ±0.2 Vrms square wave, offset by a 1 Hz, ±200 mV square wave. The transient increase/decrease has a lifetime of the order of 100 ms, and the LC response subsequently returns to its equilibrium state. As the square wave switches between positive and negative offsets, a larger amplitude is observed in the peak transmission due to the positive offset that enhances the flexoelectric effect relative to the negative offset. This transient effect confirms the screening effect predicted theoretically, and its lifetime is equal to the characteristic ion relaxation time. If the internal bias due to the different surface alignment polarities in the HAN device along with the flexoelectric polarization is of a similar order of magnitude to the external DC offset applied here, then it is reasonable to assume that the ions screen out the bias so that the remaining response is can be attributed solely to flexoelectricity for a measurement of the coefficients.

Theoretical Modelling

Ionic behaviour is implemented in the numerical model of the HAN cell by consideration of the space charge transport properties, and is drawn from a simplification of Buczkowska and Derfel's method [6, 7]. The ion concentration is determined by the generation and recombination processes. The model is based on a balance of currents due to drift and diffusion. As flexoelectricity is a bulk effect, the model can be simplified to solve the flux of ions in the bulk, using a discretization and relaxation method. Zero transport is assumed at the device boundaries, so that surface interactions can be neglected. Poisson's electrostatic equation is implemented for the potential distribution across the cell, replacing the expression in (7) to account for a non-uniform displacement field;

$$\varepsilon_0\varepsilon_\perp \frac{\partial^2 V}{\partial Z^2} + \varepsilon_0\varepsilon \cos^2\theta \frac{\partial^2 V}{\partial Z^2} - \varepsilon_0 \Delta\varepsilon \sin 2\theta \frac{\partial V}{\partial z} \cdot \frac{\partial \theta}{\partial z} + (e_1 + e_3)\cos 2\theta \left(\frac{\partial \theta}{\partial z}\right)^2 + \frac{1}{2}(e_1 + e_3)\sin 2\theta \frac{\partial^2 \theta}{\partial z^2} + \rho = 0. \tag{18}$$

where ρ is the charge density.

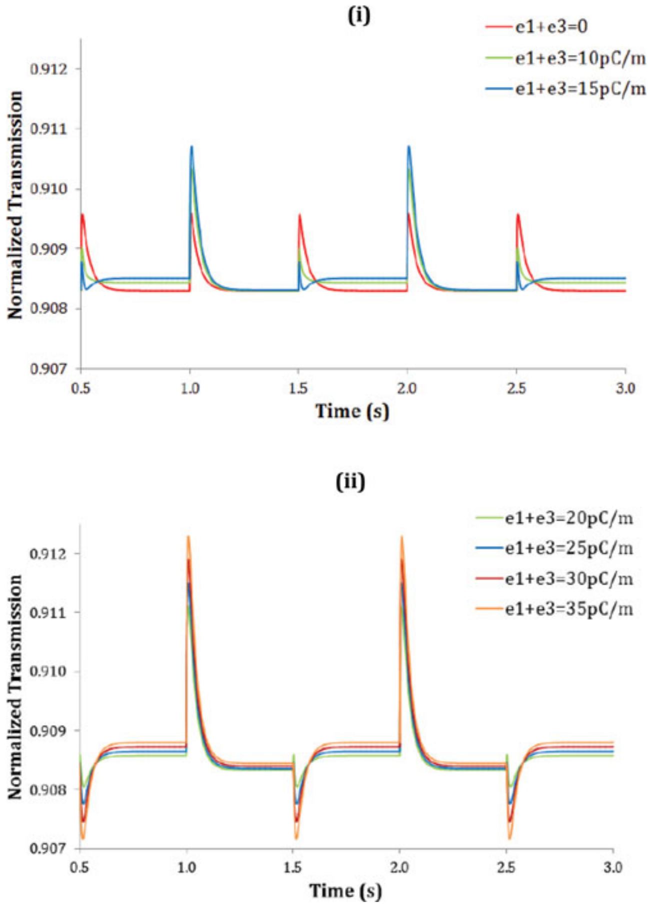

Figure 7. 1Hz, ±100 mV simulated data shows changes in amplitude and direction with variations in flexoelectric sum.

In summary, the overall model employs a finite difference technique to solve the following three main equations;

1. Euler Lagrange solution to elastic, dielectric and flexoelectric torques in the bulk.
2. Poisson's equation for potential distribution, assuming zero transport at the boundaries.
3. Continuity of ion fluxes governing transport of ions in the bulk.

The parameters varied in the data-theory fits are the generation constant in the absence of an applied field, the ion mobilities while preserving the cation to anion mobility ratio of 1.5 [6], and finally the sum of the flexoelectric coefficients. Each parameter leads to a subtle difference in the shape of each data-theory fit. Figure 7 shows an example of the transmission against time plots produced from the ionic model of the HAN cell when the flexoelectric sum is varied between 10 pCm^{-1} to 50 pCm^{-1} under the application of a 1 Hz, ±100 mVrms square wave, and for a fixed ionic content.

Data are obtained in the low frequency, low voltage perturbative regime in order to reveal the screening effect of the ions over a timescale of ∼100 ms, which is much

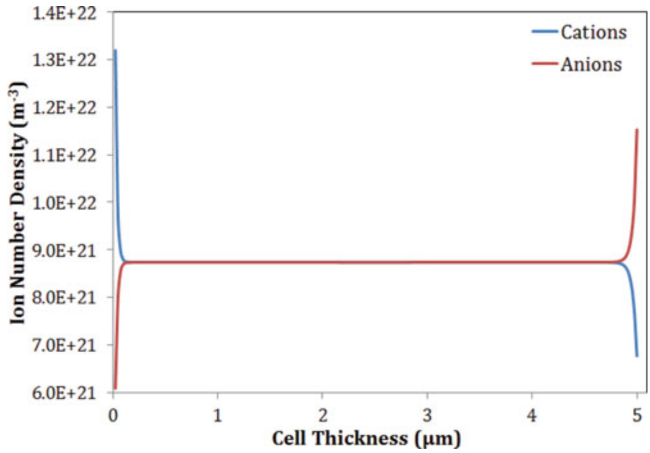

Figure 8. The data-theory fit was achieved for a high ionic content, with an average ion number density of 8.74×10^{21} m^{-3}.

faster than the wave reversal at 1 Hz. Applying low voltage signals across the device also allows the flexoelectric effect, which is linear with the applied field, to become dominant over the dielectric effect that grows quadratically in the electric field. Low values of the flexoelectric sum (up to 15 pCm^{-1}) in Fig. 7.i. produce the modulated response in the same positive direction at each wave reversal, so that the dielectric effect is predominant. This is manifested by setting $e_1 + e_3$ to zero in the model, so that the dielectric response alone produces equal amplitudes in the modulation at each wave reversal. Increasing the sum of the flexoelectric coefficients shows a change in the direction of the modulation suggesting flexoelectricity induces asymmetry in the LC response, as expected. Increasing the flexoelectric sum also shows an increase in the amplitude of the modulation, this along with the linearity of the flexoelectric effect, is exploited by obtaining data in the low voltage regime.

Results

Figure 8 shows the simulated ion number density distribution for both cations and anions. It can be seen that the ions drift to the device boundaries, with a larger distribution of positive ions at one boundary and negative ions at the other due to the different surface

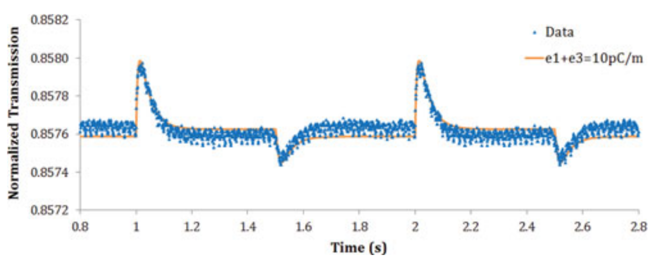

Figure 9. 1Hz, ±25 mV data-theory fit gives a flexoelectric sum of $e_1 + e_3 = 10$ pCm^{-1} for the E70 standard commerical eutectic LC mixture.

alignment polarities [4]. This ionic motion suggests that the ions do indeed drift to screen out the internal bias due to the surface polarization in a HAN device, as predicted from the preliminary experimental results in Fig. 6.

Figure 9 shows the obtained data-theory fit for transmission as a function of time from a HAN E70 nematic liquid crystal device, using the material parameters in Table I of the Appendix, under an applied field of 1 Hz, ±25 mVrms. The fit was obtained for an average ion number density of $8.74 \times 10^{21}\ m^{-3}$ in order to achieve the screening effect in the modulated LC response. A flexoelectric sum of $10 pCm^{-1}$ was obtained at this high value of the ionic content. The change in the direction of the modulated response confirms that even though a small value was measured for the sum of the flexoelectric coefficients, the flexoelectric effect is predominant at these low applied fields.

Conclusion

It is possible to measure the sum of the flexoelectric coefficients in a HAN device by exploiting highly ionic materials to ensure screening of the internal bias due to the different surface alignment polarities. A value of $|e_1 + e_3| = 10\ pCm^{-1}$ was measured in the standard commercial eutectic E70 nematic LC mixture, which is in good agreement with previous measurements of similar materials [8].

The dependency on highly ionic materials to screen out the internal bias due to surface polarization in a HAN device might be removed using different devices that have uniformly treated surface. Pi-cells in the asymmetric H state have potential to maximize the induced flexoelectric polarization on account of the asymmetric director profile; making it possible to measure the flexoelectric coefficients for a broader range of materials.

Appendix

Table I. E70 Parameters used in Numerical Model.

Property	E70 PARAMETERS	
Elastic	K_{11}	10 pN
	K_{22}	5.8 pN
	K_{33}	10.4 pN
Dielectric	$\varepsilon_{//}$	15.77
	$\varepsilon_{\perp}$	5.40
	$\Delta\varepsilon\varepsilon_0$	$91.8\ pFm^{-1}$
Birefringence	$n_{//}$	1.682
	$n_{\perp}$	1.517
	Δn	0.165

References

[1] Meyer, R. (1969). *Physics Review Letters*, *22*, 918–921.
[2] Patel, S. & Meyer, R. B. (1987). *Phys. Rev. Lett.*, *58*, 1538–1540.
[3] Ponti, S., Ziherl, P., Ferrero, C. & Zumer, S. (1999). *Liquid Crystals*, *28*, 1171–1177.
[4] Barbero, G. & Evangelista, L. R. (2003). *Physical Review E*, *68*, no. 023701, 1–2.

[5] Cornford, S. L., Taphouse, T. S. & Sambles, J. R. (2009). *New J. Phys.*, *11*, no. 013045, 13.
[6] Buczkowska, M. (2011). *Mol. Cryst. Liq. Cryst.*, *543*, 48/[814]–56/[822].
[7] Derfel, G. & Buczkowska, M. (2013). *Liquid Crystals*, *40*, 272–280.
[8] Jewell, S. A. & Sambles, J. R. (2002). *J. Appl. Phys.*, *92*, 19–24.